

THE PENNSYLVANIA STATE UNIVERSITY
SCHREYER HONORS COLLEGE

DEPARTMENT OF AEROSPACE ENGINEERING

DEVELOPMENT OF AN ADJOINT-BASED AEROELASTIC OPTIMIZER FOR TRUSS
STRUCTURES IN WINGS

ANTHONY SU
SPRING 2021

A thesis
submitted in partial fulfillment
of the requirements
for a baccalaureate degree
in Aerospace Engineering
with honors in Aerospace Engineering

Reviewed and approved* by the following:

Daning Huang
Assistant Professor of Aerospace Engineering
Thesis Advisor

Robert Melton
Professor of Aerospace Engineering
Honors Advisor

*Electronic Approvals on file.

Abstract

This thesis presents the formulation and demonstration of an adjoint-based aerostructural optimization of truss structures in wings. Aerodynamic forces are computed using strip theory aerodynamics and structural deformation is computed using a nonlinear truss solver. The wing is optimized using a gradient-based algorithm, where the gradients are solved for using the adjoint method. The adjoint method allows for extremely efficient computations of derivatives with respect to large numbers of design variables, such as the geometry of a truss. The adjoint method reduces optimization execution time by 85% compared to the finite-difference method. The computational framework developed in this study will be useful for designing 3D-printing-friendly aeroelastic models for wind tunnel testing.

Table of Contents

List of Figures	iii
List of Tables	iv
Nomenclature	v
Acknowledgements	vi
1 Introduction	1
2 Optimization Problem	3
2.1 Architecture	4
2.2 Gradient-Based Formulation	4
2.3 Adjoint Method	5
3 Structural Formulation	6
3.1 Energy Principle	6
3.2 Internal Force Vector	7
3.3 Tangent Stiffness Matrix	8
3.4 Sensitivity Matrix	8
3.5 Gradient of Objective Function	9
4 Aerodynamic Formulation	10
4.1 Aerodynamic Loads	10
4.2 Aerodynamic Sensitivity	12
5 Results	14
5.1 Structural Optimization	14
5.2 Aeroelastic Optimization	16
6 Conclusion	18
Bibliography	19

List of Figures

2.1	MDO architecture	4
4.1	Box truss in strip	10
5.1	Unoptimized box truss	15
5.2	Optimized box truss	15
5.3	Unoptimized aeroelastic wing	17
5.4	Optimized aeroelastic wing	17

List of Tables

5.1	Computational Cost of Structural Optimization	16
-----	---	----

Nomenclature

A	=	cross-sectional area
c	=	chord
C_d	=	drag coefficient
C_l	=	lift coefficient
$C_{l\alpha}$	=	lift curve slope
C_{l0}	=	lift coefficient at $\alpha = 0$
C_m	=	pitching moment coefficient
C_{m0}	=	pitching moment coefficient at $\alpha = 0$
d	=	moment arm
D	=	drag
E	=	Young's modulus
\mathbf{F}	=	internal force vector
f	=	objective function
k	=	stiffness
\mathbf{l}	=	truss member length vector
M	=	pitching moment
\mathbf{P}	=	external force vector
q	=	dynamic pressure
\mathbf{R}	=	residual function vector
S	=	wing area
U	=	energy
\mathbf{x}	=	design variable vector OR node position vector
$\hat{\mathbf{x}}$	=	truss member position vector
α	=	local angle of attack
α_0	=	global wing angle of attack
θ	=	local wing twist
ψ	=	adjoint variable
σ	=	stress
ε	=	strain
DOF	=	degree of freedom
MDO	=	multidisciplinary design optimization
NR	=	Newton-Raphson
SLSQP	=	sequential least-squares programming

Acknowledgements

I would like to thank Dr. Huang for his patience in advising this thesis project. His guidance was invaluable as I traversed my first foray into formal research.

Chapter 1

Introduction

Optimization is desirable in the design of an engineering system in order to maximize performance. Using modern computational tools, complex designs with hundreds of design variables can be optimized.

Multidisciplinary design optimization (MDO) is the application of optimization techniques to the design of a system that involves multiple disciplines. MDO enables the simultaneous, coupled analysis and optimization of many disciplines. This results in a better-optimized solution compared to sequential single-discipline optimizations, as the interactions between the disciplines can be exploited.

MDO is especially useful in the design of complex aerospace systems. In aerospace systems, there is strong coupling between disciplines such as structures, aerodynamics, thermodynamics, controls, and propulsion. Aerospace systems also have many design variables; for the aerodynamics-only shape optimization of an aircraft, there can be over 200 design variables [1]. For a more multidisciplinary optimization of the same fidelity e.g. aerostructural optimization, the number of design variables would be even larger.

Aerodynamics and structures specifically are disciplines with strong interdisciplinary coupling. Structural deformation affects the aerodynamic shape of the wing, and the aerodynamic loads on the wing determine the forces experienced by the wing's structure. Thus, aeroelastic optimization should be done with MDO to arrive at an optimal design.

In this thesis, a wing with an internal truss structure is aeroelastically optimized using the adjoint method for computing gradients. Truss structures are not common in wing spars, although experimental aircraft have flown with them [2]. While truss structures are complex and more difficult to manufacture than simple beams, the advent of accessible additive manufacturing makes rapid manufacturing of arbitrarily complex geometries possible. Thus, the rapid design/prototyping of wind tunnel models could be achieved using the framework presented here.

This thesis is organized as follows. In Chapter 2, the optimization problem is defined and the

adjoint method for computing gradients is presented. In Chapter 3, the structural model and its associated derivatives are formulated. The same is done for the aerodynamic model in Chapter 4. Then, the truss gradient solver is verified and aeroelastic optimization is demonstrated in Chapter 5. Finally, conclusions are drawn and future work is discussed in Chapter 6.

Chapter 2

Optimization Problem

In general, an optimization problem consists of a set of design variables \boldsymbol{x} , an objective function $f(\boldsymbol{x})$, and a set of constraints $\boldsymbol{g}(\boldsymbol{x})$ and $\boldsymbol{h}(\boldsymbol{x})$:

$$\begin{aligned}
 &\text{minimize} && f(\boldsymbol{x}) \\
 &\text{w.r.t.} && \boldsymbol{x} \\
 &\text{subject to} && \boldsymbol{g}(\boldsymbol{x}) \geq 0 \\
 &&& \boldsymbol{h}(\boldsymbol{x}) = 0
 \end{aligned} \tag{2.1}$$

The optimization occurs by determining the design variables that minimize the objective function while satisfying the constraints. Generally, optimization algorithms fall into one of two categories, gradient-free or gradient-based.

In a gradient-based optimization algorithm, the objective function is minimized by finding the gradient of the objective function with respect to the design parameters, $\frac{df}{dx}$. The design variables can be iteratively adjusted as to descend the objective until the gradient becomes zero and the minimum is achieved while satisfying the constraints. Generally, gradient-based methods are more efficient than gradient-free methods, and especially so for convex optimization problems with large design spaces. Although gradient-free methods can explore the design space more completely, they do not exploit gradient information efficiently.

The objective function to minimize in this thesis is the tip displacement of a wing with a box truss spar, where the geometry of the wing (and thus the size of the internal truss) is the design variable. In this study, the geometry is controlled by adjusting the widths of sections of the box truss. The optimization is subject to constraints including a constant lift generated and bounds for the truss size. The optimization algorithm used in this study is the gradient-based Sequential Least-Squares Programming (SLSQP) algorithm which is built into in the SciPy Python package [3]. The gradients are generated analytically using the adjoint method which is discussed in Section 2.3.

2.1 Architecture

The coupled aeroelastic optimization problem involves optimization, aerodynamic, and structural problems which interact with each other through intermediate variables. These interactions are shown in Fig. 2.1.

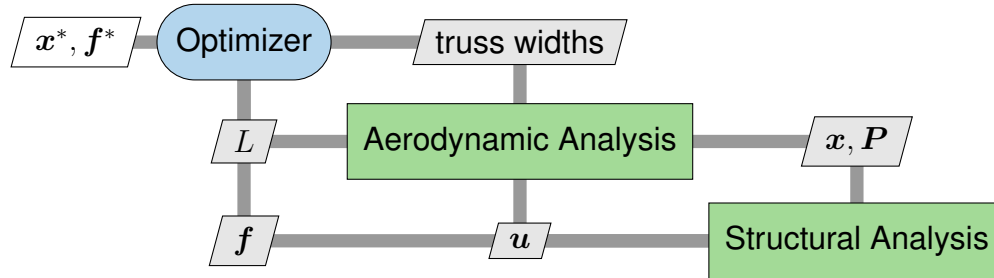


Figure 2.1: MDO architecture

Figure 2.1 was generated using the pyXDSM package [4]. The optimal parameters and objective value are denoted by \mathbf{x}^* and f^* , respectively.

2.2 Gradient-Based Formulation

In a disciplinary analysis (such as the analysis of the truss structure), the physics can be represented as a set of states \mathbf{u} that satisfy a system of equations called the residual equations.

$$\mathbf{R}(\mathbf{x}, \mathbf{u}) = 0 \quad (2.2)$$

In general, the objective function is a function of both the design variables \mathbf{x} and the system state \mathbf{u} , which is itself a function of the design variables:

$$f(\mathbf{x}, \mathbf{u}(\mathbf{x})) \quad (2.3)$$

The gradient of the objective function is thus:

$$\frac{df}{d\mathbf{x}} = \frac{\partial f}{\partial \mathbf{x}} + \frac{\partial f}{\partial \mathbf{u}} \frac{d\mathbf{u}}{d\mathbf{x}} \quad (2.4)$$

Note that $\frac{d\mathbf{u}}{d\mathbf{x}}$ is the difficult quantity to compute here if a finite-difference method is used, as it requires solving for the solution state once for each perturbation in each design variable. This would require a number of relatively expensive structural solutions proportional to the number of design variables. The other quantities in the equation are less expensive to compute, as they are partial derivatives which can be obtained while the state is held constant.

2.3 Adjoint Method

For any design variable x and corresponding feasible state u , the residuals must always be zero. Thus, the derivative of the residual function with respect to the independent variables must also be zero:

$$\frac{d\mathbf{R}}{dx} = \frac{\partial \mathbf{R}}{\partial x} + \frac{\partial \mathbf{R}}{\partial \mathbf{u}} \frac{d\mathbf{u}}{dx} = 0 \quad (2.5)$$

Equation (2.5) can be rearranged to express $\frac{d\mathbf{u}}{dx}$:

$$\frac{d\mathbf{u}}{dx} = - \left[\frac{\partial \mathbf{R}}{\partial \mathbf{u}} \right]^{-1} \frac{\partial \mathbf{R}}{\partial x} \quad (2.6)$$

Equation (2.6) can be substituted into Eq. (2.4) to produce a new expression for the gradient:

$$\frac{df}{dx} = \frac{\partial f}{\partial x} - \frac{\partial f}{\partial \mathbf{u}} \left[\frac{\partial \mathbf{R}}{\partial \mathbf{u}} \right]^{-1} \frac{\partial \mathbf{R}}{\partial x} \quad (2.7)$$

Note that the gradient can now be solved for without explicitly evaluating the costly term $\frac{d\mathbf{u}}{dx}$.

Let the adjoint variable, ψ , be

$$\psi^T = - \frac{\partial f}{\partial \mathbf{u}} \left[\frac{\partial \mathbf{R}}{\partial \mathbf{u}} \right]^{-1} \quad (2.8)$$

The adjoint variable can be obtained by solving the following linear system:

$$\left[\frac{\partial \mathbf{R}}{\partial \mathbf{u}} \right]^T \psi = - \left[\frac{\partial f}{\partial \mathbf{u}} \right]^T \quad (2.9)$$

The adjoint is substituted into Eq. (2.7) to create the following equation for the gradient:

$$\frac{df}{dx} = \frac{\partial f}{\partial x} + \psi^T \frac{\partial \mathbf{R}}{\partial x} \quad (2.10)$$

Note that after replacing $\frac{d\mathbf{u}}{dx}$, the linear system solves needed to find last term of Eq. (2.7) are the most computationally expensive step. When computing this term using the adjoint method in Eq. (2.9), this expensive linear solve has no dependence on the design variables. The cost of computing the gradient using the adjoint method scales not with the number of design variables, but with the number of outputs, which is one (the objective).

Chapter 3

Structural Formulation

This chapter presents the formulation of the nonlinear truss solver and the sensitivity matrix required for adjoint-based optimization. The truss spar consists of a set of nodes connected by members which can deform only axially.

3.1 Energy Principle

Stress and strain of a member are respectively

$$\sigma = \frac{F}{A} \quad (3.1)$$

$$\varepsilon = \frac{\Delta l}{l} \quad (3.2)$$

Assuming linear elasticity, stress and strain are related by Young's Modulus, E :

$$\sigma = E\varepsilon \quad (3.3)$$

The stress and strain of a member are uniquely defined at specific points within the beam. Thus, the internal energy of a member is given by

$$U = \int_V \frac{1}{2} \varepsilon \sigma dV \quad (3.4)$$

Assuming no change in cross section, the stress and strain can be approximated as constant across the volume of the member. Thus, the relationship becomes

$$U = \frac{1}{2} \varepsilon \sigma Al \quad (3.5)$$

This can be simplified using Eqs. (3.2) and (3.3) to become

$$U = \frac{1}{2} \frac{EA}{l} (\Delta l)^2 \quad (3.6)$$

where $k = \frac{EA}{l}$ is the effective spring stiffness of the member.

3.2 Internal Force Vector

Let a node be defined as

$$\mathbf{x} = [x_1, x_2, x_3]^T \quad (3.7)$$

In the box truss, these correspond to the x , y , and z degrees of freedom (DOF), respectively. Given a truss member defined by two nodes in space \mathbf{x}_A and \mathbf{x}_B , the initial and final positions of the member are

$$\hat{\mathbf{x}} = \begin{bmatrix} \mathbf{x}_A \\ \mathbf{x}_B \end{bmatrix} \quad (3.8)$$

$$\hat{\mathbf{x}}' = \begin{bmatrix} \mathbf{x}'_A \\ \mathbf{x}'_B \end{bmatrix} \quad (3.9)$$

The displacement of a truss member's nodes are defined by $\Delta \mathbf{x}_A$ and $\Delta \mathbf{x}_B$, respectively. The displaced nodes are

$$\mathbf{x}'_A = \mathbf{x}_A + \Delta \mathbf{x}_A \quad (3.10)$$

$$\mathbf{x}'_B = \mathbf{x}_B + \Delta \mathbf{x}_B \quad (3.11)$$

The length vectors of the initial and final truss members are

$$\mathbf{l} = \mathbf{x}_B - \mathbf{x}_A \quad (3.12)$$

$$\mathbf{l}' = \mathbf{x}'_B - \mathbf{x}'_A \quad (3.13)$$

The change in length of the truss member due to the displacement of its nodes is thus

$$\Delta l = \|\mathbf{l}'\| - \|\mathbf{l}\| \quad (3.14)$$

The internal force of the truss is found by taking the derivative of the energy with respect to the displaced nodes:

$$\mathbf{F} = k \Delta l \frac{\partial \Delta l}{\partial \mathbf{x}'} \quad (3.15)$$

Since the initial member $\|\mathbf{l}\|$ is constant, the partial derivative in Eq. (3.15) is

$$\frac{\partial \Delta l}{\partial \mathbf{x}'} = \frac{\partial \|\mathbf{l}'\|}{\partial \mathbf{x}'} = \left[\frac{\partial \|\mathbf{l}'\|}{\partial x'_{A1}} \quad \frac{\partial \|\mathbf{l}'\|}{\partial x'_{A2}} \quad \frac{\partial \|\mathbf{l}'\|}{\partial x'_{A3}} \quad \frac{\partial \|\mathbf{l}'\|}{\partial x'_{B1}} \quad \frac{\partial \|\mathbf{l}'\|}{\partial x'_{B2}} \quad \frac{\partial \|\mathbf{l}'\|}{\partial x'_{B3}} \right]^T \quad (3.16)$$

where

$$\frac{\partial \|\mathbf{l}'\|}{\partial x_{Ai}} = - \left((x'_{B1} - x'_{A1})^2 + (x'_{B2} - x'_{A2})^2 + (x'_{B3} - x'_{A3})^2 \right)^{-\frac{1}{2}} (x'_{Bi} - x'_{Ai}) \quad (3.17)$$

$$\frac{\partial \|\mathbf{l}'\|}{\partial x_{Bi}} = - \left((x'_{B1} - x'_{A1})^2 + (x'_{B2} - x'_{A2})^2 + (x'_{B3} - x'_{A3})^2 \right)^{-\frac{1}{2}} (x'_{Bi} - x'_{Ai}) \quad (3.18)$$

for $i = 1, 2, 3$. Combining Eqs. (3.15) to (3.18), the internal force vector is

$$\mathbf{F} = \frac{EA}{\|\mathbf{l}\|} \frac{\Delta l}{\|\mathbf{l}'\|} \begin{bmatrix} -\mathbf{l}' \\ \mathbf{l}' \end{bmatrix} \quad (3.19)$$

3.3 Tangent Stiffness Matrix

The truss displacement is found by solving the following equilibrium equation, i.e. the residual equations:

$$\mathbf{R}(\mathbf{u}) = \mathbf{F}(\mathbf{u}) - \mathbf{P}(\mathbf{u}) = 0 \quad (3.20)$$

where \mathbf{P} is the external force vector and the state \mathbf{u} is the shape of the deformed structure. Equation (3.20) is solved using Newton-Raphson (NR) iteration. In NR iteration, an initial guess for the solution to the residual equations is iterated on using the method in Eq. (3.21). The iteration continues until the residual equations are satisfied to within a tolerance.

$$\begin{aligned} \mathbf{u}_{n+1} &= \mathbf{u}_n + \Delta \mathbf{u} \\ \text{where } \Delta \mathbf{u} &= - \left[\frac{\partial \mathbf{R}}{\partial \mathbf{u}} \right]^{-1} \mathbf{R}(\mathbf{u}_n) \end{aligned} \quad (3.21)$$

This iteration requires the Jacobian $\frac{\partial \mathbf{R}}{\partial \mathbf{u}}$, which is found by taking the derivative of the residual equations with respect to the state:

$$\frac{\partial \mathbf{R}}{\partial \mathbf{u}} = \frac{\partial \mathbf{F}}{\partial \mathbf{u}} - \frac{\partial \mathbf{P}}{\partial \mathbf{u}} \quad (3.22)$$

The external forcing component $\frac{\partial \mathbf{P}}{\partial \mathbf{u}}$ is derived later in Section 4.2. The internal force component $\frac{\partial \mathbf{F}}{\partial \mathbf{u}}$ is the tangent stiffness matrix. The tangent stiffness matrix is found by taking the second derivative of the energy of the element given in Eq. (3.6):

$$\frac{\partial \mathbf{F}}{\partial \mathbf{u}} = \frac{\partial^2 U}{\partial \mathbf{u}^2} = \frac{EA}{\|\mathbf{l}\|^2} \left(1 - \frac{\|\mathbf{l}\|}{\|\mathbf{l}'\|} \right) \begin{bmatrix} \mathbf{I} & -\mathbf{I} \\ -\mathbf{I} & \mathbf{I} \end{bmatrix} + \frac{EA}{\|\mathbf{l}\| \|\mathbf{l}'\|^3} \mathbf{u} \mathbf{u}^T \quad (3.23)$$

The tangent stiffness matrix for the whole truss is a larger matrix assembled from these element tangent stiffness matrices. This stiffness matrix can then be used in NR iteration to solve for the structure state of the truss \mathbf{u} .

3.4 Sensitivity Matrix

It is evident in Eq. (2.9) that computing the adjoint variable requires the Jacobian $\frac{\partial \mathbf{R}}{\partial \mathbf{x}}$, which is the sensitivity matrix. Using Eq. (3.20), the sensitivity matrix is found as having two components:

$$\frac{\partial \mathbf{R}}{\partial \mathbf{x}} = \frac{\partial \mathbf{F}}{\partial \mathbf{x}} - \frac{\partial \mathbf{P}}{\partial \mathbf{x}} \quad (3.24)$$

The external forcing component $\frac{\partial \mathbf{P}}{\partial \mathbf{x}}$ is derived later in Section 4.2.

The internal force component of the sensitivity matrix takes the form of a 6×6 square matrix:

$$\frac{\partial \mathbf{F}}{\partial \mathbf{x}} = \begin{bmatrix} \frac{\partial \mathbf{F}}{\partial x_{A1}} & \frac{\partial \mathbf{F}}{\partial x_{A2}} & \frac{\partial \mathbf{F}}{\partial x_{A3}} & \frac{\partial \mathbf{F}}{\partial x_{B1}} & \frac{\partial \mathbf{F}}{\partial x_{B2}} & \frac{\partial \mathbf{F}}{\partial x_{B3}} \end{bmatrix} \quad (3.25)$$

The i th component of the j th partial derivative in Eq. (3.25) is

$$\frac{\partial F_{x_i}}{\partial x_j} = -2EA \frac{l'_i l_j}{\|\mathbf{l}\|^3} \quad (3.26)$$

Simplifying and combining all terms of the internal force sensitivity matrix in the form of a vector equation yields

$$\frac{\partial \mathbf{F}}{\partial \mathbf{x}} = \frac{-2EA}{\|\mathbf{l}\|^3} \begin{bmatrix} \mathbf{l}' \\ -\mathbf{l}' \end{bmatrix} [\mathbf{l} \quad -\mathbf{l}] \quad (3.27)$$

3.5 Gradient of Objective Function

Recall from Section 2.3 that the gradient takes the form

$$\frac{df}{d\mathbf{x}} = \frac{\partial f}{\partial \mathbf{x}} + \boldsymbol{\psi}^T \frac{\partial \mathbf{R}}{\partial \mathbf{x}} \quad (2.10)$$

$$\boldsymbol{\psi}^T = -\frac{\partial f}{\partial \mathbf{u}} \left[\frac{\partial \mathbf{R}}{\partial \mathbf{u}} \right]^{-1} \quad (2.8)$$

The objective function's sensitivity to the design variables $\frac{\partial f}{\partial \mathbf{x}}$ is zero, because the objective function (tip deflection) depends only on the final structural state and not the design variables. $\frac{\partial f}{\partial \mathbf{u}}$ is a unit vector in the vertical DOF of the tip node, because the objective function is equal to just the vertical deflection at the tip node. Thus, the gradient can be found using these vectors and the quantities derived in Sections 3.3, 3.4, and 4.2.

Chapter 4

Aerodynamic Formulation

4.1 Aerodynamic Loads

Let the wing be discretized span-wise into strips, each of which contain a single box of the box truss spar. The box contains eight nodes in the arrangement shown in Fig. 4.1. Note that diagonal truss members exist on each face of the box, but are omitted in the figure for clarity.

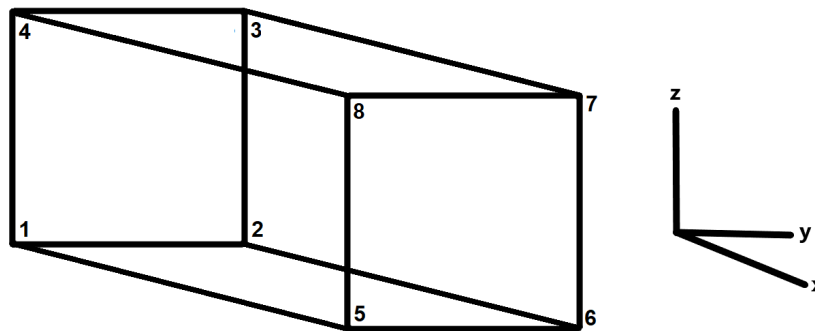


Figure 4.1: Box truss in strip

The positive x -direction is the spanwise direction and the positive y -direction points to the trailing edge of the wing. In this chapter, the DOF of a node previously denoted by $[x_1, x_2, x_3]$ will instead be denoted by $[x, y, z]$ for clarity, and numerical subscripts instead denote the node.

Each of the wing strips acts as wing section in its own two-dimensional flow. Each strip has its unique chord, span, deflection, and angle of attack. All wing strips share the same freestream flow.

For a wing strip spanning from y_1 to y_2 , the relevant aerodynamic quantities can be calculated by

$$L = \int_{y_1}^{y_2} qcC_l dy \quad (4.1)$$

$$D = \int_{y_1}^{y_2} qcC_d dy \quad (4.2)$$

$$M = \int_{y_1}^{y_2} qc^2 C_m dy \quad (4.3)$$

If it is assumed that the geometry and aerodynamic forces change linearly in the span-wise direction, then the above equations for panel loads become

$$L = qc\Delta y C_l \quad (4.4)$$

$$D = qc\Delta y C_d \quad (4.5)$$

$$M = qc^2\Delta y C_m \quad (4.6)$$

In this study, the lift is modelled as having a linear relationship with α and the pitching moment coefficient about the aerodynamic center is modelled to be constant:

$$C_l = C_{l0} + C_{l\alpha}\alpha \quad (4.7)$$

$$C_m = C_{m0} \quad (4.8)$$

The drag coefficient is approximated to be zero, although future development work could implement a more accurate quadratic relationship with dynamic pressure and lift coefficient.

Another notable assumption in this aerodynamic model is that wing strips act as if in 2-D flows, i.e. spanwise flow and other induced effects are not present. This increases the overall root bending moment, as the lift calculated near the wing tips is greater than that in reality.

When the wing twists, the local angle of attack changes. This twist angle can be added to the wing angle of attack to find the local angle of attack. This twist angle can be measured by finding the slope between two initially horizontal truss nodes.

The local angle attack of a point on the wing is thus

$$\alpha = (\alpha_0 + \theta) \cos(\beta) \quad (4.9)$$

The equation for lift L gives the force in the wind axes. If the initial angle of attack of the wing is non-zero, the forces must be converted to the equivalent forces in the global frame L' and D' :

$$L' = \cos(\alpha_0)L - \sin(\alpha_0)D \quad (4.10)$$

$$D' = \sin(\alpha_0)L + \cos(\alpha_0)D \quad (4.11)$$

Note that the wing bending is not part of this transformation because wing bending is assumed to be small. It is also assumed that α_0 is a small angle. Thus,

$$L' \approx L \quad (4.12)$$

$$D' \approx D = 0 \quad (4.13)$$

These lift loads are then distributed evenly across the internal structure's truss nodes. The forces due to twisting moment must also be evenly distributed between the nodes of the strip. First, the distance d between each of the nodes and the aerodynamic center must be found. If the box truss spar is centered on the aerodynamic center undergoing small deformations, this distance is approximately equal to half of the width of the spar. The force on the node can then be found by solving

$$\mathbf{M}_{\text{local}} = \frac{\mathbf{M}}{8} = \mathbf{F} \times \mathbf{d} \quad (4.14)$$

Note that the vector result of Eq. (4.14) will always point in the spanwise (positive x) direction if bending is assumed to be small.

4.2 Aerodynamic Sensitivity

This section describes the sensitivity of the external aerodynamic force vector to the structure state $\frac{\partial \mathbf{P}}{\partial \mathbf{u}}$, but this method applies to the sensitivity of force vector to the initial structure geometry $\frac{\partial \mathbf{P}}{\partial \mathbf{x}}$ also. Thus, to compute the sensitivity with respect to the initial structure geometry, the following method is repeated with \mathbf{x} in place of \mathbf{u} .

The sensitivity can be broken down into components due to lift and pitching moment, respectively:

$$\frac{\partial \mathbf{P}}{\partial \mathbf{u}} = \frac{\partial \mathbf{P}_L}{\partial \mathbf{u}} + \frac{\partial \mathbf{P}_M}{\partial \mathbf{u}} \quad (4.15)$$

Changes in the forces from moments on truss nodes can be due to changing total moment on the wing strip or due to changing moment arm of the truss node d (node distance from aerodynamic center or truss center). Thus, the second derivative in Eq. (4.15) can be decomposed using the chain rule:

$$\frac{\partial \mathbf{P}}{\partial \mathbf{u}} = \frac{\partial \mathbf{P}_L}{\partial \mathbf{u}} + \frac{\partial \mathbf{P}_{\dot{M}}}{\partial \mathbf{u}} d + \frac{\partial \mathbf{P}_d}{\partial \mathbf{u}} M \quad (4.16)$$

where $\frac{\partial \mathbf{P}_{\dot{M}}}{\partial \mathbf{u}} d$ represents the change in \mathbf{P}_M due to changes in total moment where moment arm is held constant, and $\frac{\partial \mathbf{P}_d}{\partial \mathbf{u}} M$ represents the change in \mathbf{P}_M due to changes in moment arm where total moment is held constant.

The lift derivative $\frac{\partial \mathbf{P}_L}{\partial \mathbf{u}}$ changes with wing area and with twist angle, both of which are direct functions of components of \mathbf{u} . Eq. (4.17) shows the load on a single node.

$$P_{L,i} = \frac{C_{l\alpha} dq (-y_8 + y_7 + y_6 - y_5 - y_4 + y_3 + y_2 - y_1) \left(\frac{y_7 - y_8}{z_7 - z_8} + \frac{y_6 - y_5}{z_6 - z_5} + \frac{y_5 - y_4}{z_5 - z_4} + \frac{y_2 - y_1}{z_2 - z_1} \right)}{16t} \quad (4.17)$$

The total moment derivative $\frac{\partial \mathbf{P}_{\dot{M}}}{\partial \mathbf{u}} l$ also changes with wing area. Note that in Eq. (4.18) d is held constant for the purposes of derivatives.

$$P_{\dot{M},i} = \frac{C_m dq (-y_8 + y_7 + y_6 - y_5 - y_4 + y_3 + y_2 - y_1)^2}{16dt} \quad (4.18)$$

The moment arm derivative $\frac{\partial d}{\partial \mathbf{u}} M$ changes with box truss width, which is once again a direct function of components of \mathbf{u} . Note that, unlike in Eqs. (4.17) and (4.18), this is not the same

between the two sides of the wing strip. Also note that in the following equations M is held constant for the purposes of derivatives.

$$P_{d,i} = \begin{cases} 2M/(y_1 - y_0) & \text{if } i = 1, 2, 3, 4 \\ 2M/(y_5 - y_4) & \text{if } i = 5, 6, 7, 8 \end{cases} \quad (4.19)$$

Substituting the above terms for $\frac{\partial P_L}{\partial u}$, $\frac{\partial P_M}{\partial u}$, and $\frac{\partial d}{\partial u}$ into Eq. (4.16) yields the full form of the aerodynamic force sensitivity.

Chapter 5

Results

This chapter covers the results of verification tests and the aeroelastic optimization of the wing.

5.1 Structural Optimization

In this section, the adjoint-based gradient implementation is verified. A single-discipline structural optimization using the adjoint method of computing the gradient is demonstrated and compared to the finite-difference method for computing the gradient. In this structure-only optimization, the load condition was set to a constant load at the tip of the truss and the derivatives were adjusted accordingly. The aeroelastic lift constraint was replaced with a mass constraint: the mass was constrained to be no greater than the mass of the initial truss. The bounds for the truss width design variables were set to $[0.05, 10]$. For this test, the box truss consisted of 4 boxes. Each box had an initial width of 1 and a fixed length of 1.

The optimized truss reduced tip displacement by 0.008, or 40%, compared to the initial truss. The resultant trusses of the optimization are shown in Figures 5.1 and 5.2. The dashed red lines indicate initial position of the truss and the solid green lines indicate the final deformed state of the structure.

The optimized truss has a wide root and tapers continuously to the tip. This is because bending near the root results in a larger tip deflection than bending near the tip. Thus, the optimization resulted in the width distribution of the truss which best managed the trade-off between bending stiffness at the root and at the tip.

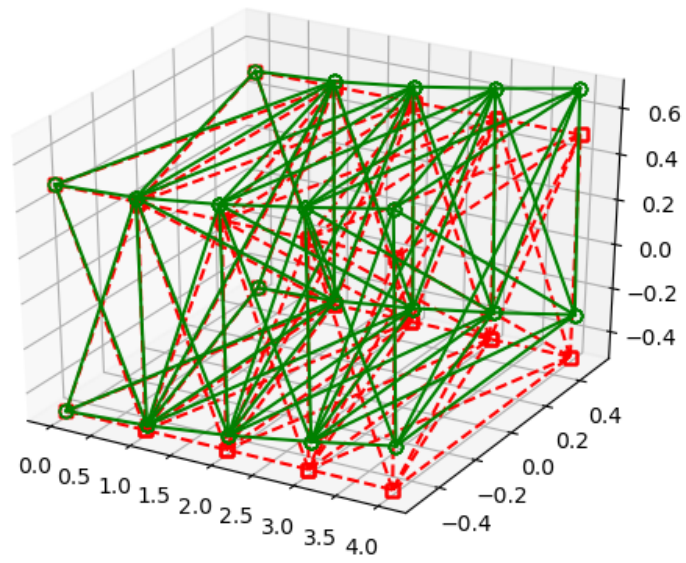


Figure 5.1: Unoptimized box truss with tip displacement $\delta = 0.020$

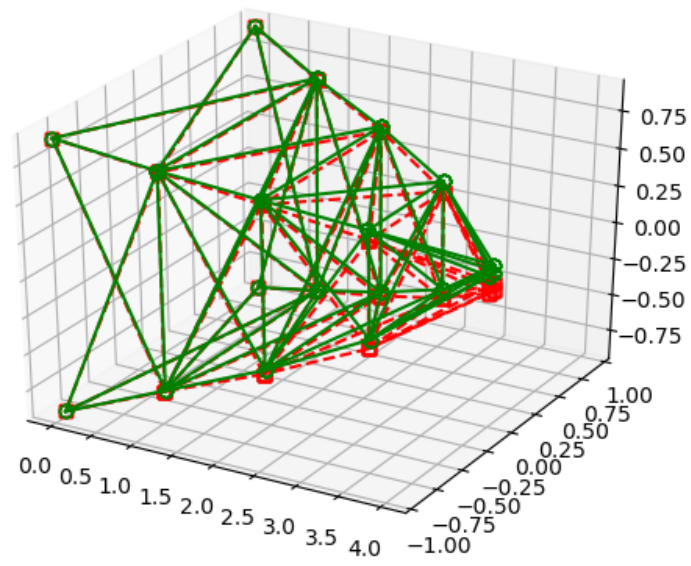


Figure 5.2: Optimized box truss with tip displacement $\delta = 0.012$

The same optimization was also performed using a two-point finite-difference numerical gradient. The results of the adjoint-based and finite-difference optimizations are shown in Table 5.1. The execution times were obtained on a single core of an Intel Core i7-8550U processor in a consumer-grade laptop system.

Table 5.1: Computational Cost of Structural Optimization

	Adjoint-Based Gradient	Finite-Difference Gradient
tip displacement	0.012	0.012
execution time (s)	96	645
iterations	25	25
function evaluations	26	176

While both methods of computing the gradient resulted in a converged optimization, the use of an adjoint-based analytical gradient reduced execution time by 85% compared to the finite-difference gradient run. This is due to the finite-difference gradient requiring a large number of function calls, and thus a large number of expensive structural solves.

5.2 Aeroelastic Optimization

In this section, the optimization of the aeroelastic wing is demonstrated. For this optimization, the box truss consisted of 5 boxes. The bounds for the truss width design variables were set to $[0.25, 4]$. These bounds are more restrictive than the truss-only problem in order to simulate a real wing with a minimum and maximum thickness requirement due to the size of aircraft systems and the wing-fuselage junction, respectively. Each box had an initial width of 1 and a fixed length of 5.

This optimization test assumed a constant wing load throughout deformation. Thus, the load sensitivity to structure state is assumed to be zero.

The optimized aeroelastic wing reduced tip deflection by 0.0115, or 83%, compared to the initial wing. The resultant truss spars of the optimization are shown in Figures 5.3 and 5.4. Note that since the thickness ratio of the wing is constant, the wing's chord distribution is proportional to the truss' width distribution.

One interesting feature of this optimized truss spar is that its surface is concave near the root and convex near the tip, while the surface of the optimized fixed-load truss is convex throughout. Since a wing strip's aerodynamic loads are proportional to its area, and thus its width, the aeroelastically optimized truss has a large structure (and thus aerodynamic load) near the root of the wing. This reduces the bending moment the wing experiences and thus reduces the tip displacement while still maintaining high lift.

One other feature to note is the apparent discontinuity of the smooth box truss width distribution at $x = 5$. This is due to the truss width bounds defined in the optimization problem; the upper limit for the width was reached.

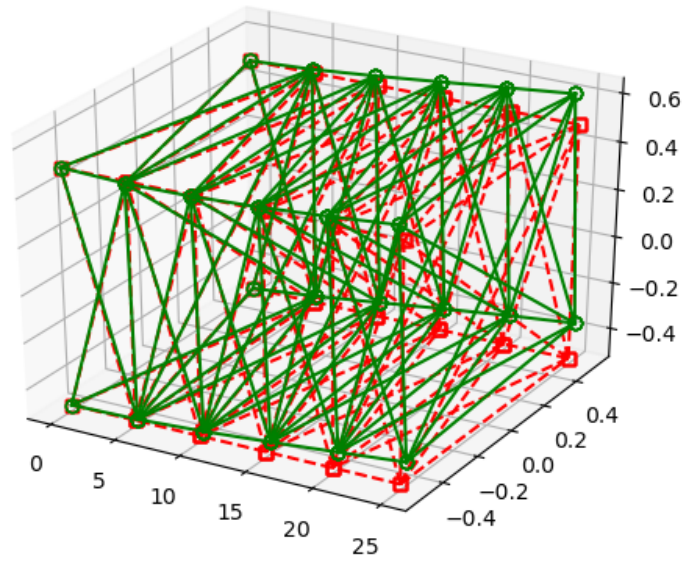


Figure 5.3: Unoptimized aeroelastic wing with tip displacement $\delta = 0.0139$

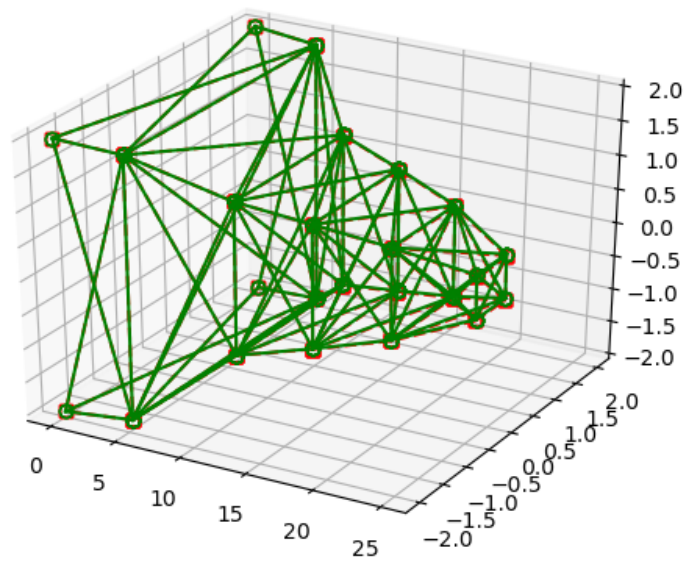


Figure 5.4: Optimized aeroelastic wing with tip displacement $\delta = 0.0024$

Chapter 6

Conclusion

This thesis presented a computational framework for the aeroelastic optimization of a wing with truss structures. An implementation of the adjoint-based optimization was shown to reduce computational cost compared to the reference finite-difference case, and the aeroelastic optimization of a wing was demonstrated.

From a practical perspective, there is much more work to be done before the method described in this thesis can be used to design a real model. The implementation of the aeroelastic wing must be generalized such that more design flexibility is afforded, e.g. placement of the spar at a point other than the aerodynamic center. The fidelity of the structural and aerodynamic models also need to be upgraded if any application with highly flexible wings is desired.

Bibliography

- [1] Lyu, Z., Xu, Z., and Martins, J. R. R. A., “Benchmarking Optimization Algorithms for Wing Aerodynamic Design Optimization,” *Proceedings of the 8th International Conference on Computational Fluid Dynamics*, Chengdu, Sichuan, China, July 2014, ICCFD8-2014-0203.
- [2] Jordan, S., DeGraw, T., Mahon, M., Murphy, G., Chopra, I., and Nagaraj, V. T., “Development and Flight Testing of the Gamera-S Solar Powered Helicopter,” 2017.
- [3] Kraft, D., “A Software Package for Sequential Quadratic Programming,” Tech. Rep. DFVLR-FB 88-28, DLR German Aerospace Center – Institute for Flight Mechanics, Koln, Germany, 1988.
- [4] Lambe, A. B. and Martins, J. R. R. A., “Extensions to the Design Structure Matrix for the Description of Multidisciplinary Design, Analysis, and Optimization Processes,” *Structural and Multidisciplinary Optimization*, Vol. 46, 2012, pp. 273–284.

ACADEMIC VITA - ANTHONY SU

EDUCATION

B.S. in Aerospace Engineering August 2018 - May 2021
The Pennsylvania State University, University Park, PA

- Schreyer Honors College
- Thesis: Development of an Adjoint-Based Aeroelastic Optimizer for Truss Structures in Wings

WORK/PROJECT EXPERIENCE

Lead Design Engineer August 2020 - May 2021
PSU Design-Build-Fly

- Managed team of six members in design and documentation of model airplane
- Performed preliminary analysis and trade studies for conceptual design of model airplane
- Performed aerodynamic and performance calculations
- Developed multidisciplinary design optimization code for aircraft sizing

Materials Research Intern August 2020 - May 2021
Collins Aerospace, Windsor Locks, CT

- Designed experiments to validate repeatability of additive manufacturing processes
- Characterized additively manufactured materials
- Created builds for laser powder bed fusion (LPBF) machinery
- Wrote standard operating procedures for additive manufacturing processes

Payload Subsystem Lead August 2019 - May 2021
SEDS @ Penn State

- Coordinated design requirements and constraints with systems engineering lead
- Led CAD design, construction, and verification of rocket payload
- Managed general body members in construction of payload

Computer-Aided Design Lead August 2019 - May 2020
PSU Design-Build-Fly

- Performed full CAD design of all model airplane systems
- Assisted chief engineer in performing and documenting performance/aerodynamic analyses
- Manufactured wet-layup composite structures

Maker-In-Residence (Part-Time) November 2018 - November 2019
Pennsylvania State University, University Park, PA

- Harvested and maintained a 3D printer farm
- Provided consultations for students learning to 3D model or 3D print
- Demonstrated creative uses of 3D printing and other rapid prototyping tools

HONORS AND AWARDS

PSU Engineering Design Showcase: People's Choice Award 2018
President's Freshman Award 2018
Dean's List 2018 - Present
National Merit Scholarship Finalist 2018

PROFESSIONAL MEMBERSHIPS

Student Member - American Institute of Aeronautics and Astronautics 2019 - Present